NOTE

A Study on γ-Fe_2O_3 Loaded Poly(methyl methacrylate) Nanocomposites

N. N. Mallikarjuna,[1] A. Venkataraman,[2] T. M. Aminabhavi[1]

[1]*Center of Excellence in Polymer Science, Karnatak University, Dharwad, 580 003, India*
[2]*Department of Chemistry, Gulbarga University, Gulbarga, 585106, India*

Received 7 May 2004; accepted 7 July 2004
DOI 10.1002/app.21144
Published online in Wiley InterScience (www.interscience.wiley.com).

INTRODUCTION

Over the past decade, a flurry of research activity has occurred in producing polymeric nanocomposites by incorporating inorganic nanoparticles.[1] The unique properties of nanoparticles are due to quantum-confinement or surface effects that become operative on the nanoscale.[2] Since the pioneering work of Gleiter,[3] innumerable studies have been made to understand the physicochemical aspects of nanocomposites.[4–7] A variety of metal oxides could be dispersed into poly(methyl methacrylate) (PMMA), to produce nanocomposites with enhanced mechanical strength and thermal stability together with the ease of processibility and flexibility.[8–11] In this note, we report the usefulness of γ-Fe_2O_3 nanoparticles prepared by the combustion method[12,13] to prepare nanocomposite films of PMMA by the solvent casting method. These materials have been characterized by X-ray diffraction (XRD), Fourier transform infrared (FTIR), scanning electron microscopy (SEM), and thermal analysis techniques, viz., thermogravimetric analysis (TGA) and differential thermal analysis (DTA). The nanocomposites show increased thermal stability as the amount of γ-Fe_2O_3 in the PMMA matrix increased.

EXPERIMENTAL

Materials

Poly(methyl methacrylate), ferrous chloride, chloroform, acetone, ferric acetylacetonate, and polyethylene glycol-4000 were all of reagent grade samples purchased from S. D. Fine Chemicals, Mumbai, India.

Preparation of nanocomposite films

The γ-Fe_2O_3 nanoparticles in the size range of 10–100 nm were prepared using the combustion method proposed earlier.[12,13] In brief, ferric acetylacetonate was mixed with polyethylene glycol-4000 in the mass ratio of 1 : 5 and ground to produce uniform size particles in a pestle and mortar. The resultant solid was taken in a silica crucible and heated in air. Initially, polyethylene glycol was melted, frothed, and finally ignited to form γ-Fe_2O_3 nanoparticles. Upon cooling to room temperature, no traces of carbon impurities were left in the final residue of γ-Fe_2O_3

A known mass of PMMA was dissolved in 100 mL of chloroform and the mixture was kept for 12 h for complete dissolution. The solution was transferred to a rotary evaporator. The γ-Fe_2O_3 powder 2, 5, and 10 mass % was taken in chloroform and sonicated. It was then mixed with PMMA in solution in a rotary evaporator maintained at 80°C. Chloroform was evaporated by vacuum at 200 rpm. The derived nanocomposites were designated as PMMA-2, PMMA-5, and PMMA-10 to represent 2, 5, and 10 mass % of the dispersed γ-Fe_2O_3, respectively. Pure PMMA is designated as PMMA-0.

RESULTS AND DISCUSSION

In the present study, nanocomposite films of PMMA loaded with varying amounts of γ-Fe_2O_3 were prepared by evaporating chloroform in a rotary evaporator. The XRD data presented in Figure 1(a) revealed a sharp peak at $2\theta = 42^o$ due to the crystalline nature of γ-Fe_2O_3. After incorporation of γ-Fe_2O_3 nanoparticles into PMMA matrix, the observed sharp peak is masked, indicating a molecular level dispersion of γ-Fe_2O_3 into the PMMA matrices [see Figs. 1(b)—(d)]. Similar observations are seen for pure PMMA matrix due to its noncrystalline nature [see Fig. 1 (d)].

FTIR studies have been performed to understand the possible chemical interactions between γ-Fe_2O_3 and PMMA. FTIR spectra of pure PMMA displayed in Figure 2 (d) is quite different from those of γ-Fe_2O_3 loaded nanocomposites [Figs. 2(a)—(c)]. The characteristic peak at 371 cm^{-1} in

This article is CEPS Communication #47.
Correspondence to: T. M. Aminabhavi (aminabhavi@yahoo.com).

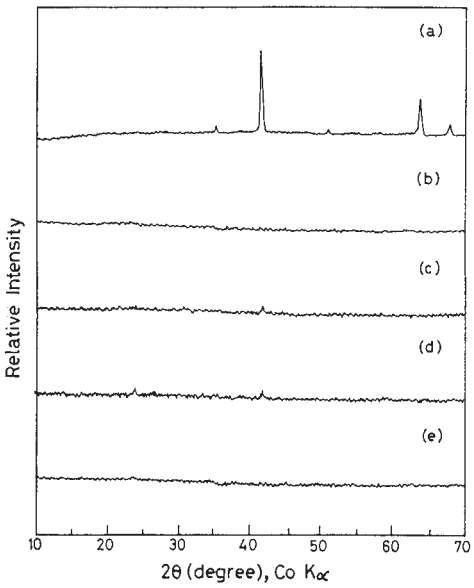

Figure 1 XRD tracings of (a) pure γ-Fe_2O_3, (b) PMMA-2, (c) PMMA-5, (d) PMMA-10, and (e) PMMA-0 nanocomposite films.

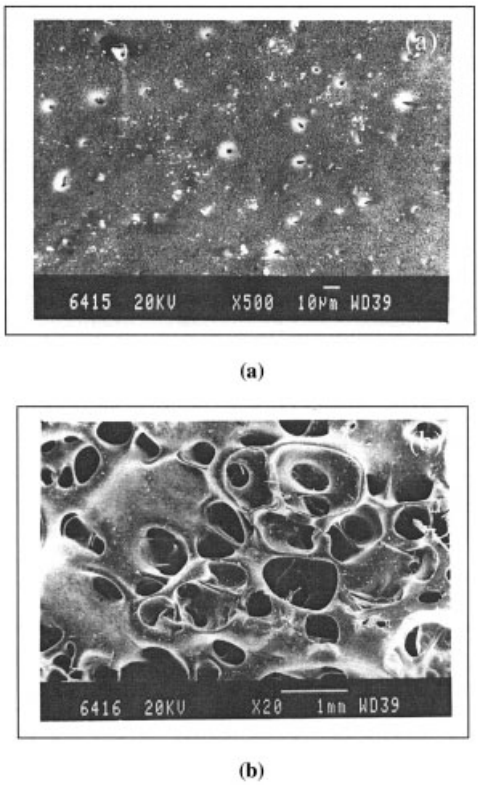

Figure 3 SEM photographs at (a) low resolution and (b) high resolution for PMMA-2 nanocomposite films.

pure PMMA is absent in all the composites. Similarly, the characteristic peaks observed at 445 and 550 cm^{-1} for γ-Fe_2O_3 due to Fe–O vibrations have disappeared in all the composite films. However, a slight shift in peak observed at 550 cm^{-1} in all the nanocomposites compared to PMMA-0 [see Figs. 2(b)—(d)] may be due to the possible H-bond type interactions between γ-Fe_2O_3 nanoparticles and PMMA.

Morphology of the nanocomposites studied by SEM at low and high resolutions are presented, respectively, in Figures 3(a) and (b) for PMMA-2. At high resolution [Fig. 3(b)], the deformation of PMMA is prevalent with a neck-like structure.[14] Similar and more elongated structures are also observed in PMMA-5 and PMMA-10 nanocomposites as shown in Figures 4(a) and (b) and 5(a) and (b) both at low and high resolutions, respectively. Thus, it appears that by adding higher amounts of γ-Fe_2O_3 greater deformation of

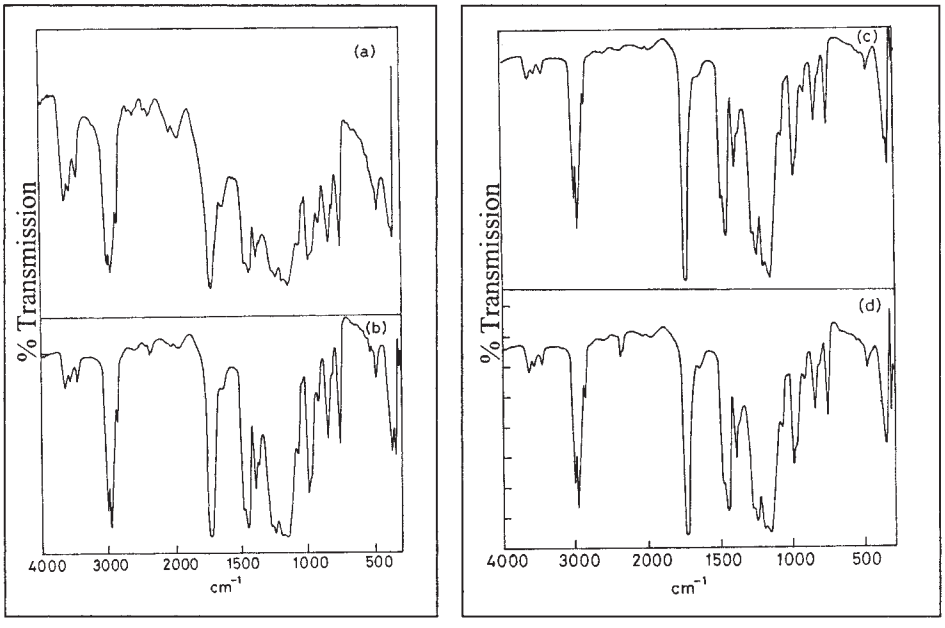

Figure 2 FTIR Spectra of (a) PMMA-0, (b) PMMA-2, (c) PMMA-5, and (d) PMMA-10 nanocomposite films

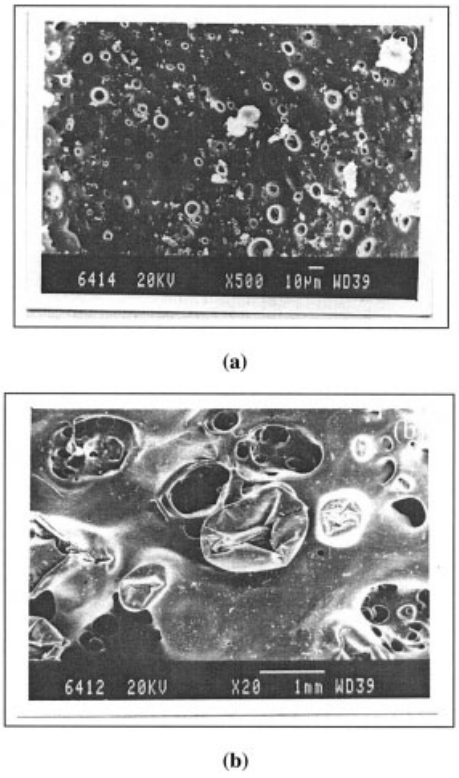

Figure 4 SEM photographs at (a) low resolution and (b) high resolution for PMMA-5 nanocomposite films.

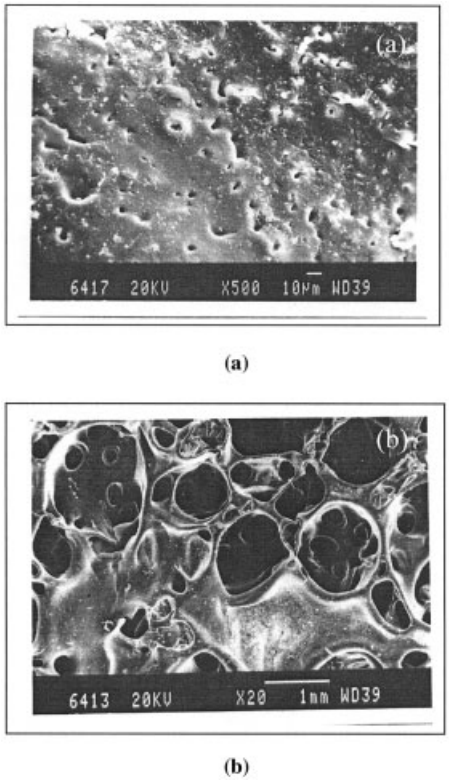

Figure 5 SEM photographs at (a) low resolution and (b) high resolution for PMMA-10 nanocomposite films.

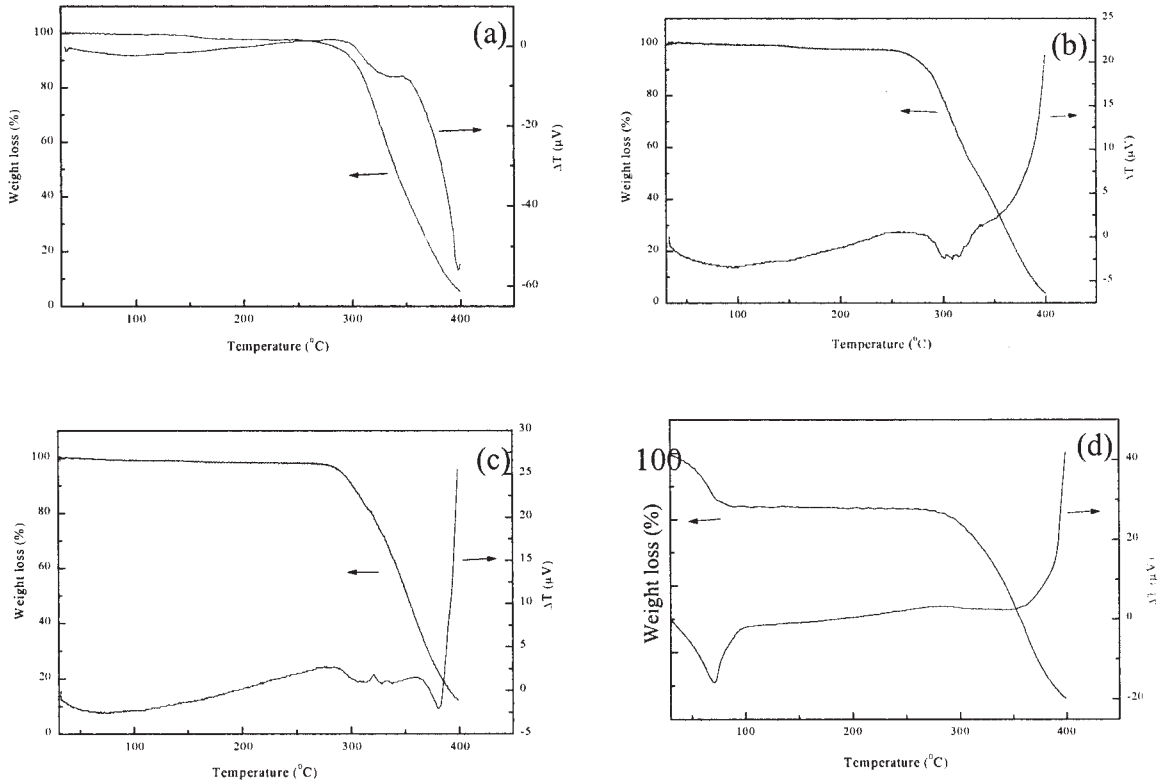

Figure 6 TGA/DTA tracings of (a) PMMA-0, (b) PMMA-2, (c) PMMA-5, and (d) PMMA-10 nanocomposite films.

the PMMA matrix is possible due to increased filling of the pores in the matrix.

In an effort to understand the thermal properties of nanocomposites, both TGA and DTA experiments have been performed on pure PMMA and γ-Fe_2O_3 loaded nanocomposite films. The TGA tracing of pure PMMA shows stability up to 300°C, which starts to degrade at 315°C, showing a continuous weight loss [see Fig. 6(a)]. For PMMA-2 films, TGA tracings [see Fig. 6(b)] indicate that degradation temperature is identical to pure PMMA ($\sim$ 315°C). DTA curves show a hump at 270°C, possibly due to phase transition of γ-Fe_2O_3 to α-Fe_2O_3. Thus, there is not much improvement in the thermal stability in PMMA-2, but, in PMMA-5, the TGA curve [Fig. 6(c)] shows the onset of decomposition temperature around 330°C. On the other hand, TGA/DTA curves for the PMMA-10 sample displayed in Figure 6(d) indicate increased thermal stability with a highest degradation temperature of 380°C. However, a dip observed at 75°C may be due to the presence of moisture in the sample. It is well known that γ-Fe_2O_3 nanoparticles absorb moisture and, since PMMA-10 contains a higher amount of γ-Fe_2O_3, higher moisture content is present in PMMA-10. This is also confirmed by TGA.

CONCLUSION

Preliminary results of this study indicate that it is possible to disperse nanoparticles of γ-Fe_2O_3 into PMMA matrix. Further, the thermal stability of nanocomposites increase with an increasing amount of γ-Fe_2O_3. The synthesis of γ-Fe_2O_3 by the combustion method is unique since the nanoparticles can be obtained in the size range of 10–100 nm in a single step in a few minutes. However, other methods available in the literature involve a multistep process and particles in nanosize range are difficult to obtain. However, our interest is to study the effect of the addition of γ-Fe_2O_3 on the thermal stability of the nanocomposite. Other property measurements such as magnetic and electrical data are in progress.

References

1. Caruso, F. Adv Mater 2001, 13, 11.
2. Henglein, A. Chem Rev 1989, 89, 1861.
3. Gleiter, H. Adv Mater 1992, 4, 474.
4. Hahn, H. Nanostructured Mater 1997, 9, 3.
5. Vollath, D.; Szabo, D. V. Nanostructured Mater 1994, 3, 927.
6. Wang, Y. Z., Qiao, G. W., Lu, X. D.; Ding, B. Z.; Hu, Z. Q.; Mater Lett 1993, 17, 152.
7. Vollath, D.; Szabo, D. V.; Taylor, R. D.; Willis, J. O. J Mater Res 1997, 12, 2175.
8. Xavier, J. L. L.; Guyot, A.; Bourgeat-Lami, E. J Colloid Interface Sci 2002, 250, 82.
9. Ash, B. J.; Schadler, L. S.; Siegel, R.W. Mater Lett 2002, 55, 83.
10. Zeng, J.; Sattysiak, B.; Johnson, W. S.; Schiraldi, D. A.; Kumar, S. Composites 2004, B35, 173.
11. Tatro, S.R.; Clayton, L. M.; O'Rourke Muisener, P.A., Rao, A. M., Harmon, J. P. Polymer 2004, 45, 1971.
12. Mallikarjuna, N. N.; Venkataraman, A. Ind J Eng Mater Sci 2003, 10, 50.
13. Mallikarjuna, N. N.; Lagashetty, A.; Govindaraj, B.; Venkataraman, A. J Therm Anal Calor 2003, 71, 915.
14. Kargin, V. A. International Symposium on Macromolecular Chemistry; Butterworth & Co (Pub) Ltd.: London, 1965; Chap. 1.